Review article

Nahid Talebi[a,*], Surong Guo[a] and Peter A. van Aken

Theory and applications of toroidal moments in electrodynamics: their emergence, characteristics, and technological relevance

https://doi.org/10.1515/nanoph-2017-0017
Received January 30, 2017; revised June 21, 2017; accepted July 9, 2017

Abstract: Dipole selection rules underpin much of our understanding in characterization of matter and its interaction with external radiation. However, there are several examples where these selection rules simply break down, for which a more sophisticated knowledge of matter becomes necessary. An example, which is increasingly becoming more fascinating, is macroscopic toroidization (density of toroidal dipoles), which is a direct consequence of retardation. In fact, dissimilar to the classical family of electric and magnetic multipoles, which are outcomes of the Taylor expansion of the electromagnetic potentials and sources, toroidal dipoles are obtained by the decomposition of the moment tensors. This review aims to discuss the fundamental and practical aspects of the toroidal multipolar moments in electrodynamics, from its emergence in the expansion set and the electromagnetic field associated with it, the unique characteristics of their interaction with external radiations and other moments, to the recent attempts to realize pronounced toroidal resonances in smart configurations of meta-molecules. Toroidal moments not only exhibit unique features in theory but also have promising technologically relevant applications, such as data storage, electromagnetic-induced transparency, unique magnetic responses and dichroism.

Keywords: toroidal moment; multipole expansion; radiation pattern; metamaterial; spin; coupling.

1 Introduction

Although the history of Maxwell equations and light-matter interaction started as early as 1861 [1], electromagnetism has been the field of most challenging and rival concepts such as understanding the actual velocity of the information transfer [2], the actual wave function of photons [3–5], realization of cloaking, negative refraction, and transferring of the data beyond the diffraction limits using plasmons and metamaterials [6–11], and the emergence of the Abraham-Minkowski controversy and the actual linear momentum of light [12, 13]. At the heart of our understanding of light-matter interaction, there exist multipole-expansion sets that tell us how to construct the *extended* electromagnetic sources according to the localized sources with well-known electromagnetic field and radiation patterns. This concept, for example, forms the basics to understand the quasi-static dipole and quadrupole localized plasmon resonances in individual [14] or chains of metallic nanoparticles arranged in the forms of converter-coupler gratings [15], waveguides [16–18], or resonators [19, 20] (the so-called longitudinal and transverse resonances). The coefficients of such an expansion set known as moments were conventionally ordered as appearing in the expansion set according to the electric and magnetic multipole terms.

In 1958, however, Zeldovich [21] reported on the possibility of elementary particles under breakdown of spatial parity to interact with the electromagnetic wave in a peculiar form considering the interaction energy $H^{\text{int}} = -\vec{S}\cdot\vec{\nabla}\times\vec{H}$, where $\vec{S}$ is the spin and $\vec{H}$ is the magnetic field. Considering this problem in classical electrodynamics, in 1967, Dubovik noticed the possibility of introducing a new class of moments being excluded from the family of electric and magnetic moments, with different time-space symmetries but appearing in similar orders in the expansion set to the magnetic moments [22], the so-called toroidal moments. From those early days, discussions about toroidal moment have created an impetus in both solid-state physics and electrodynamics.

[a]**Nahid Talebi and Surong Guo:** These authors contributed similarly to this work.
***Corresponding author: Nahid Talebi,** Max Planck Institute for Solid State Research, Heisenbergstr. 1, 70569 Stuttgart, Germany, e-mail: n.talebi@fkf.mpg.de
Surong Guo and Peter A. van Aken: Max Planck Institute for Solid State Research, Heisenbergstr. 1, 70569 Stuttgart, Germany

Open Access. © 2017 Nahid Talebi et al., published by De Gruyter. BY-NC-ND This work is licensed under the Creative Commons Attribution-NonCommercial-NoDerivatives 4.0 License.

What is so interesting about toroidal moments? This question is partly entangled with the human curiosity to find new states of matter and ordering and partly related to the technological applications. Toroidal ordering in solid states can open up possibilities for a new kind of magnetoelectric phenomenon [23], with applications in data storage and sensing. Whereas toroidal moments have been reviewed in Ref. [23], with a focus on static spin-based toroidal moments and magnetoelectric effect (ME) in condensed-matter physics, we will put the emphasis of our review on different expansion sets leading to the toroidal moment and on electrodynamic toroidal moments in metamaterials and free space. Ref. [24] has provided a concise review in this aspect. Our review is intended to provide a more complete answer to this question and to invoke new directions in light-matter interactions involving toroidal moments. For this purpose, we start with the theoretical investigation of the multipole expansion sets in Section 2 leading to toroidal moments and time-space symmetry characteristics of moments, respectively. We furthermore discuss in Section 3 the toroidal moments in solid-state and photonic systems, the origin of asymmetric magnetoelectric tensors in materials, the electromagnetic interaction between external light and (meta-)materials that sustain toroidal moments, and finally the electromagnetic field and radiation pattern associated to isolated toroidal moments. In Section 4, we further consider the possibility of the excitation of materials with toroidal moments with different polarization states of light and also with relativistic electrons. In Section 5, we explore the coupling of toroidal moments to other classes of moments like electric dipole to form radiation-free sources of electromagnetic fields and also discuss the characteristics of toroidal metamaterials. We continue the review to cover the technological applications of toroidal moments and finally provide a conclusion and an outlook.

2 Families of multipoles in electrodynamics

Mathematical expansion sets are essential for our understanding of the physical properties of systems and matter. Not only such expansion sets help us to analytically find solutions to simple problems, but they also help us to simplify or find approximate solutions to complicated systems. Among the so-called expansion sets that physicists routinely use are Rayleigh expansion sets [10, 25], Eigenmode expansion sets [11, 26, 27], and multipole expansion sets [28]. The multipole expansion, which is based on the expansion of either potentials [29–31] or fields [32, 33], has several applications in classical electrodynamics, such as finding solutions to inverse problems [34–36], reconstruction of images [37], and in general, decomposition of induced charges into a set of localized charge distributions with well-known near-field and far-field characteristics. Moreover, semianalytical methods based on multipole expansion sets of magnetic and electric vector potentials, such as the method of auxiliary sources [38–40], the multiple multipole method [41–43], or the generalized multipole technique [11, 18, 44–49], are exponentially convergent efficient methods in numerical electromagnetics [50]. In the following, we consider the family of multipole expansions for static and dynamic systems, considering the Taylor expansions of sources, potentials and fields.

2.1 Multipole expansions for potentials and fields

A direct Taylor expansion of charge and current densities proposed by Dubovik in 1990 already demonstrated the existence of a toroidal moment described as $\vec{T} = (1/10c)\int(\vec{r}\,\vec{r}\cdot\vec{J}(\vec{r}) - 2r^2\vec{J}(\vec{r}))d^3r$, which originates from the currents flowing along the meridians of an infinitesimal sphere as $\vec{J}_T = \vec{\nabla}\times(\vec{\nabla}\times(\vec{T}\delta(\vec{r})))$. $\vec{J}(\vec{r})$ then continues as the inner flow by extending from one pole to the other pole of the sphere [22, 51] (see Figure 1A). Moreover, toroidal moment was shown to be a multipole order originated from the transverse part of the current density $\vec{J}_\perp(\vec{r}, t)$, as the longitudinal current $(\vec{J}_\parallel(\vec{r}, t))$ is not independent from the charge density, because of the charge conservation criterion $\vec{\nabla}\cdot\vec{J}_\parallel(\vec{r}, t) = -\partial\rho(\vec{r}, t)/\partial t$ and hence is related to the multipole expansion of the scalar potential. Here, the longitudinal current is associated with the irrotational part of the current density vector field and points out from the charge density $\rho(\vec{r}, t)$ toward a direction normal to any surface inclosing the charge distribution, whereas $\vec{J}_\perp(\vec{r}, t)$ is parallel to such a surface. Obviously, a configuration of the current density distribution in the form of $\vec{J}_T$ is topologically similar to the poloidal currents flowing at the surface of a torus, hence leading to toroidal magnetic fields and the so-called polar toroidal moment (see Figure 1B). Interestingly, the poloidal current distribution leads to a diminishing of the magnetic quadrupole moment and hence an increase in the detectability of toroidal moment [52]. As a simplification, a ring of either static [23, 53] or dynamic [54–57] magnetic moments is considered as a configuration for the excitation of a polar toroidal moment or the so-called magnetic toroidal moment.

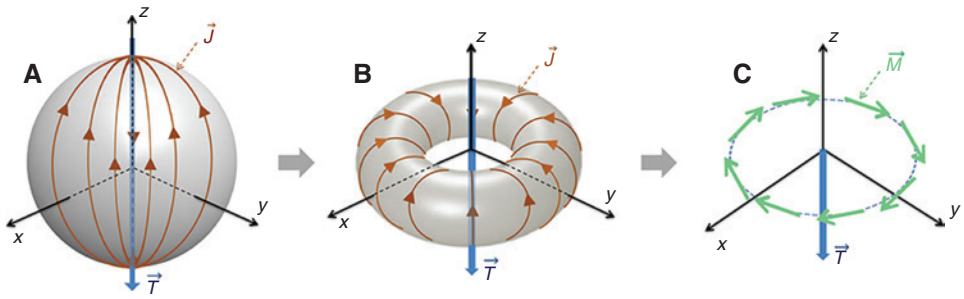

Figure 1: Current density and magnetic moment distributions associated with the toroidal moment.
Poloidal currents excited at the surface of (A) a sphere and (B) a toroid. (C) Equivalently, a ring of magnetic moments is also attributed to the excitation of a toroidal moment.

A dual configuration to the polar toroidal moment is an axial toroidal moment (or electric toroidal moment), which is composed of a ring of electric dipolar configurations [51, 58]. However, in contrast to a polar (magnetic) toroidal moment, the axial (electric) toroidal moment does not violate time and parity symmetry. In this paper, we mainly focus on the polar (magnetic) toroidal moment.

More often, the solutions to potentials rather than field components are considered. This is based on the fact that solutions of the Helmholtz equations, known as wave potentials, are well established in arbitrary coordinate systems. Moreover, it is possible to form a Helmholtz equation for potentials in complicated materials like chiral and topological materials [59], which is not in general feasible for field components. In addition, these are the vector $\vec{A}(\vec{r}, t)$ and the scalar $\varphi(\vec{r}, t)$ potentials, which more often appear in the quantum mechanical Hamiltonian of the interaction of charged particles with light. However, scalar and vector potentials are also not independent, where a gauge theory should be applied to pursue a physically relevant wave solution for electromagnetic fields [60]. In practice, considering each gauge, theory dictates a relation between the scalar and vector potentials, meaning that they are not independent. Hence, the multipoles obtained by expanding them are also not independent. Considering the Lorentz gauge as $\vec{\nabla}\cdot\vec{A}(\vec{r}, t) = -(1/c)\partial\varphi(\vec{r}, t)/\partial t$, the longitudinal part of the vector potential is also determined by the scalar potential. In other words, multipole expansion sets related to the scalar potential or the longitudinal part of the vector potential, along with the transverse part of the vector potential, form a complete basis of multipoles. Following Vrejoiu [29], the reduction of the multipole tensors in the form of symmetric traceless ones demonstrates the existence of a toroidal moment, which has the same order as the magnetic quadrupole moment, but sustains different symmetry rules. This is, however, in contrast to the static case, for which no toroidal moment is obtained even after a tedious reduction of the tensors according to the symmetry groups. Therefore, the family of toroidal moments is composed of hybrid moments, which only come to existence by expanding the transverse part of the vector potential. In this regard, the toroidal dipole and quadrupole tensors in Cartesian coordinate and in Gaussian units are obtained as

$$T_i = \frac{1}{10c}\int [r_i(\vec{r}\cdot\vec{J}(r, t)) - 2r^2 J_i(r, t)]d^3r \tag{1}$$

$$T_{ik} = \frac{1}{42c}\int 4r_i r_k(\vec{r}\cdot\vec{J}(\vec{r}, t)) - 5r^2(r_i J_k + r_k J_i) + 2r^2(\vec{r}\cdot\vec{J}(\vec{r}, t)\delta_{ik})d^3r, \tag{2}$$

where $i, k \in (x, y, z)$ and δ_{ik} is the Kronecker-delta function. It should be noted that, often, an equivalent definition of the toroidal moment is considered as $\vec{T} = (1/6c)\int \vec{r}\times(\vec{r}\times\vec{J}(\vec{r}, t))\, d^3r$ (the toroidal moment is the moment of the dipole-magnetic moments), which has an equivalent time-averaged quantity to the one which was introduced in Eq. (1).

Additionally, a direct expansion of fields may be also exploited, for which the outgoing-wave Green's function is expanded versus spherical harmonic multipoles [61]. Incorporating the Helmholtz decomposition of the current density function into the longitudinal and transverse toroidal and poloidal terms [31], the resulting electric field has three components as $\vec{E}(\vec{r}, \omega) = -\vec{\nabla}e^L(\vec{r}, \omega) - \vec{r}\times\vec{\nabla}e^T(\vec{r}, \omega) - \vec{\nabla}\times(\vec{r}\times\vec{\nabla}e^P(\vec{r}, \omega))$ where e^L, e^T and e^P are its Debye scalar potentials associated with longitudinal, toroidal and poloidal currents, respectively. In this regard, toroidal currents produce toroidal electric and poloidal magnetic fields, and poloidal currents produce poloidal electric and toroidal magnetic fields.

In a different approach, Spaldin et al. [62] have introduced the magnetization density $\vec{\mu}(\vec{r})$ in a solid state system and its interaction energy with the external magnetic field as $H_{\text{int}} = -\int \vec{\mu}(\vec{r}) \cdot \vec{H}(\vec{r}) d^3r$, where $\vec{\mu}(\vec{r})$ can have contributions from both spin and orbital momentum. They further have expanded the magnetic field in powers of the field gradient to conclude moment distributions in the form of (i) the net magnetic moment of the system $(\vec{m} = \int \vec{\mu}(\vec{r}) d^3r)$, (ii) the pseudo-scalar quantity called magnetoelectric monopole $(a = (1/3)\int \vec{r} \cdot \vec{\mu}(\vec{r}) d^3r)$, (iii) the toroidal moment vector dual to the antisymmetric part of the tensor $(\vec{t} = (1/2)\int \vec{r} \times \vec{\mu}(\vec{r}) d^3r)$, and (iv) the quadruple magnetic moment of the system $(q_{ij} = (1/2)\int [r_i \mu_j + r_j \mu_i - (2/3)\delta_{ij} \vec{r} \cdot \vec{\mu}(\vec{r})] d^3r)$, to name only the first few terms in the expansion set. The interaction energy can be further expanded as $H_{\text{int}} = -\vec{m} \cdot \vec{H}(\vec{r}=0) - a(\vec{\nabla} \cdot \vec{H})_{\vec{r}=0} - \vec{t} \cdot (\vec{\nabla} \times H)_{\vec{r}=0} - \sum_{ij} q_{ij} (\partial_i H_j + \partial_j H_i)_{\vec{r}=0}$, where i, j are Cartesian directions and δ_{ij} is the Kronecker-delta function.

As a summary, all kinds of multipole expansion techniques can be introduced, but decomposition techniques should be exploited to extract the toroidal order, with the symmetry specifications discussed in the following chapter.

2.2 Classification of multipoles according to symmetry rules

In a Maxwell-Lorentz system of equations in which the only sources are charges and currents related to each other as $\vec{J} = \sum e_i \vec{v}_i \delta(\vec{r} - \vec{r}_i)$, electric, magnetic and toroidal moments form a complete system of moments and there is no place for further generalizations. However, for the sake of completeness and symmetry, consideration of magnetic charges is recommended as well [63], as $\vec{\nabla} \cdot \vec{B}(\vec{r}, t) = \rho_g(\vec{r}, t)$ and $\vec{\nabla} \times \vec{E}(\vec{r}, t) = -(\partial \vec{B}(\vec{r}, t)/\partial t) - \vec{J}_g(\vec{r}, t)$, where $\rho_g(\vec{r}, t)$ and $\vec{J}_g(\vec{r}, t)$ are magnetic charge and magnetic current density distributions, respectively and $\vec{E}(\vec{r}, t)$ and $\vec{B}(\vec{r}, t)$ are the electric and magnetic flux components, respectively, at time t and position shown by the displacement vector $\vec{r}$. Moreover, in contrast to the electric current distribution, which is a vector, the magnetic current distribution is an axial vector (pseudo-vector). Generalizing the multipole expansion schemes to include magnetic sources, a new class of poloidal magnetic currents is unraveled, which gives rise to the axial (electric) toroidal moments, which is an exact dual to the polar (magnetic) toroidal moment discussed previously. In analogy to the work carried out in Ref. [51], the axial (electric) toroidal moments are denoted here as G. Under space-time parity operations (space inversion and time reversal), the whole class of multipoles behaves as depicted in Table 1. The symmetry rules should be applicable to the vector fields acting on the multipoles, as the free energy of the system should be invariant upon space-time inversions. In this regard, the free energy of the interaction of an arbitrary system with the electromagnetic field in free-space is given by $\vec{H}_{\text{int}} = -\vec{P} \cdot \vec{E} - \vec{T} \cdot (\partial \vec{D}/\partial t) - \vec{M} \cdot \vec{H} - \vec{G} \cdot (\partial \vec{B}/\partial t)$ [64]. Moreover, Spaldin et al. [23] have argued that the cross-product $\vec{P} \times \vec{M}$ sustains similar space-time symmetries as a toroidal moment, but in fact, it is not a toroidal moment, as it interacts with the electromagnetic field according to the free-energy term $(\vec{P} \times \vec{M}) \cdot (\vec{E} \times \vec{H})$. We only mention here that the local distribution of the vector $\vec{r} \times \vec{M}(\vec{r}) = \vec{r} \times (\vec{r} \times \vec{J}(\vec{r}))$ can be described as the distribution of the toroidal moment, when only the time-averaged quantity of this vector is anticipated and compared to $(\vec{r}\,\vec{r} \cdot \vec{J}(\vec{r}) - 2r^2 \vec{J}(\vec{r}))$, as described in Section 3.1. Moreover, as it will be discussed later in this review, a linear ME might occur in a system with a net toroidal moment, which means that the free-energy function contains the contribution $\vec{T} \cdot (\vec{E} \times \vec{H})$ [22].

Although parity considerations in space-time is believed to provide a complete class of multipoles, a more general picture beyond the quasi-static limits has to be considered when the retardation effects are taken into account [65], in which the Taylor expansion versus the wave number (k) is included as well. As this expansion is always ruled out versus $k^2 = (\omega/c)^2$ in free space, there is no room to discuss momentum-frequency symmetries in classical electrodynamics. However, considering induced currents in materials, anisotropic media, and also material losses, it is well known that time-reversal symmetries might be violated in special cases [66]. In this regard, a complete picture including the k-symmetry has to be developed.

To conclude this section, we mention that despite several experimental realizations of toroidal moments in both solid-state and metamaterials systems, there are still debates about an individual class of toroidal moments,

Table 1: Transformation properties of electric (P), magnetic (M), polar toroidal (T), and axial toroidal (G) moments under space inversion and time reversal operations.

Multipole	Parity	
	Space	Time
P	−	+
M	+	−
T	−	−
G	+	+

to be excluded from the magnetic quadrupole terms. An interesting study in this regard is presented in Ref. [67], where the author has considered multipole expansions at both potential and field levels, but also in both Cartesian and spherical coordination.

3 Characteristics, interaction, and radiation of toroidal moment in materials

3.1 Toroidization and ME in materials

A static toroidal moment exists in various materials both microscopically and macroscopically, covering transition metal ions [68], biological and chemical macromolecules [69–74], bulk crystals [75–80], and glasses [81]. In macroscopic condensed matter, formation of toroidal moments in materials plays a vital role in the asymmetric ME. ME describes a phenomenon of a spontaneous magnetization (polarization) induced by an external electric (magnetic) field. The effect can be linear or nonlinear (higher order), having symmetric or antisymmetric tensors, and usually depends on temperature. An antisymmetric tensor is described by $[\xi]^{\mathrm{T}} = -[\xi]$, where T is transpose operator. Moreover, an antisymmetric tensor is a special case of an asymmetric tensor where the latter is described by $\xi_{ij} \neq \xi_{ji}$. One consequence of the antisymmetric linear ME in materials is toroidization, which is denoted by forming an order of vortices of the spontaneously induced magnetization [80] or spin [23].

In solid-state systems where the magnetic fields are induced by localized spins $(\vec{S}_\alpha)$ at sites $\vec{r}_\alpha$, the toroidal moment can be derived as $\vec{T} = (g\mu_B/2)\sum_\alpha \vec{r}_\alpha \times \vec{S}_\alpha$, with the gyromagnetic ratio g and the Bohr magneton μ_B. However, toroidal moments have origin-specific values related to the choice of the lattice [82]. By shifting the origin from $\vec{r}$ to $\vec{r}' = \vec{r} + \vec{R}_0$, the toroidal moment changes as $\vec{T}' = \vec{T} + (g\mu_B/2)\left(\vec{R}_0 \times \sum_\alpha \vec{S}_\alpha\right)$. In contrast to the moment, changes in toroidization (toroidal moment per volume of unit cell) are uniquely defined values. Nevertheless, as for the ferroelectric materials, spontaneous toroidization can be defined in materials with net toroidal moments, which describes the rate of change in toroidal moments when a vector field is applied. In general, symmetry considerations hint at the contribution of toroidal moments to the magnetoelectric polarization when considering the free energies of systems with spin ordering and the electrodynamics Hamiltonian of systems showing the linear ME. However, toroidal moments are not the only source of the ME. It is almost impossible to provide a direct relation between toroidization and magnetoelectric coupling [23]. Nonequilibrium electrodynamic consideration can describe the differences in the off-diagonal magnetoelectric tensors below a critical temperature, which is related to the coupling between the spontaneous toroidization, magnetization, and polarization [83–85]. In general, the antisymmetric contribution to the magnetoelectric tensor is an indication for the presence of toroidization in materials.

Ferrotoroidicity describes a spontaneous, long-range alignment of toroidal moments in materials. It has been of major interest to investigate whether the ferrotoroidicity consisting of magnetic toroidal moments can be defined as an individual class of ferroic state, in addition to ferroelastic, ferromagnetic, and ferroelectric orders [23, 53, 80, 86, 87]. The reason is that the ferrotoroidicity complements the others in terms of space-time-inversion symmetry, whose transformation property is characterized by changing sign under both time reversal and spatial inversion. In this sense, ferrotoroidic state in materials is expected to be dominant like other primary order parameters. Zimmermann et al. [53] demonstrated for the first time the hysteretic switching of ferrotoroidic domains in $LiCoPO_4$, where they simultaneously applied crossed static magnetic and electric fields. They concluded that the ferrotoroidic order is a primary order parameter as other ferroic states.

It has been further discussed that the toroidal moment might be merely a vortex-like arrangement of magnetic moments from antiferromagnetic state. Tolédano et al. [80] proposed a case study of $LiFeSi_2O_6$ in this aspect. All the magnetoelectric tensor components during the symmetry-breaking transition from monoclinic to triclinic magnetic phase at 18 K in $LiFeSi_2O_6$ were measured. In terms of crystallographic symmetry, either a biquadratic coupling of the toroidal-moment vector components or the antiferromagnetic vector components is permitted and is able to explain the observed inversion symmetry breaking. However, in terms of microscopic physics, only the free energy of the toroidal coupling term can be large enough to drive the transition in a single step. This is due to the fact that the free-energy contribution from the antiferromagnetic vector components is geometrically attenuated. Therefore, to distinguish ferrotoroidicity from ferromagnetic order in a material, it is necessary to examine both the crystallographic symmetry and the collective response of the associated moments.

As mentioned previously, in systems with nonvanishing magnetic moments the toroidal moment depends

on the choice of origin [82]. It was suggested to choose an origin for which the system is centrosymmetric and nontoroidal in the initial configuration. The change of toroidal moment is then derived from a symmetry-breaking structure distortion at the final state and thus can be interpreted as the spontaneous toroidal moment of the system [82]. Ferrotoroidicity has been demonstrated by materials whose magnetic order breaks spatial inversion symmetry. It is waiting for exploration in a variety of material systems and holds a great potential for future applications [86].

Experimental characterization of ferrotoroidic states requires a probe and a detection mechanism that violates space-time symmetry. Obviously, the measurement of magnetoelectric coefficients is an appropriate but indirect method for investigating toroidal moments in materials, as was achieved for $Co_3B_7O_{13}Br$ [83] and Cr_2O_3 only when it starts to be driven into the spin-flop phase [88]. Moreover, the magnetoelectric tensor of Cr_2O_3 sustains also a relativistic-invariant pseudoscalar term [89], which is associated with the axionic ME [90] and the so-called Tellegen term [91].

Considering the magnetic insulator $LiCoPO_4$ and the *XY*-like spin glass $Ni_xMn_{1-x}TiO_3$ ($x \approx 0.42$) as examples, $LiCoPO_4$ has a net toroidal moment T (0, T_y, T_z) $\neq 0$ below 21.8 K [53]. The predominant component T_z of the toroidal moment is induced by two pairs in Co^{2+} (each pair highlighted in purple or green in Figure 2A), while the other component T_y caused by spin rotation away from the *y*-axis is approximately two orders of magnitude smaller and thus can be neglected [53]. For the ilmenite structure of the *XY*-like spin glass $Ni_xMn_{1-x}TiO_3$ ($x \approx 0.42$), the Ni^{2+} and Mn^{2+} ions are randomly distributed in the magnetic (Ni, Mn) plane and form a honey comb lattice. At the presence of the cross-product of the electric and magnetic field components, a net toroidal moment is polarized in the direction perpendicular to the honeycomb lattices during the spin-freezing process (in Figure 2B) [81].

Apart from toroidization in bulk material at low temperatures, toroidization might be achieved at room

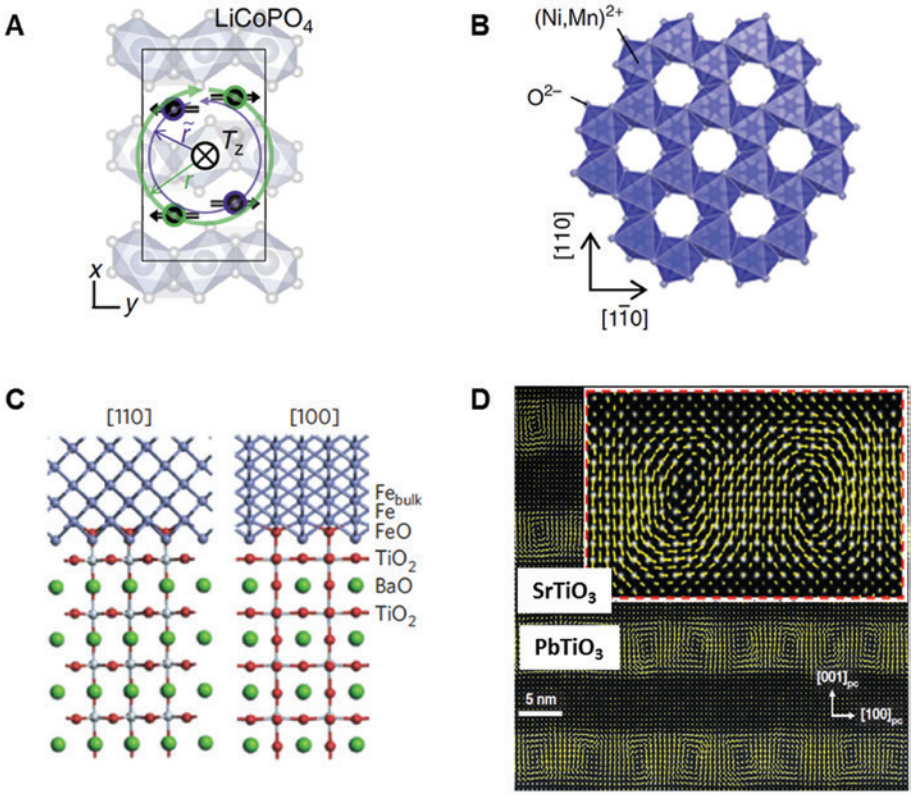

Figure 2: Examples of toroidal moment in materials.
(A) Z-component of the toroidal moment in $LiCoPO_4$ originated from two spin pairs in Co^{2+} shown for its magnetic unit cell (rectangle) [53]. Because of the different radii $\tilde{r} < r$, the clockwise and counterclockwise contributions from these two pairs do not cancel. (B) Crystal structure of $Ni_xMn_{1-x}TiO_3$ projected along the hexagonal *c* axis [001] [81]. (C) Structural model of the interface type (-Fe-FeO-TiO_2-$BaTiO_3$) between Fe and $BaTiO_3$ [92]. (D) An array of vortex-antivortex pairs present in each $PbTiO_3$ layer indicated by polar displacement vectors (yellow arrows) [93]. Figures reproduced with permission from (A) Ref. [53], NPG; (B) Ref. [81], NPG; (C) Ref. [92], NPG; (D) Ref. [93], NPG.

temperature by interface engineering due to structural modification, charge transfer and strain effects [92, 93]. Figure 2C shows one possible interface type of (-Fe-FeO-TiO_2-$BaTiO_3$) between Fe and $BaTiO_3$, which results in a spontaneous magnetization and polarization at room temperature. Polar vortices for electric toroidal moment are observed in oxide superlattices ($SrTiO_3$ and $PbTiO_3$) [93], as shown in Figure 2D. However, in the experiments mentioned here, where the spatial-temporal symmetry was broken with a strong correlation across the interface, it is the quantity $\vec{P}\times\vec{M}$ which contributes to the detected time-averaged signal.

3.2 Interaction of optical waves with toroidized materials

Optical waves are used to detect the long-range order of toroidization in materials, but not for producing toroidization. Moreover, if any detection method should be used for recognizing ferrotoroidic orders, it should sustain odd parity and odd time-reversal symmetries. An example of an optical effect with such symmetry considerations is gyrotropic birefringence [94, 95], which is also called nonreciprocal directional dichroism (NDD) [96] (see Figure 3A). NDD appears in materials with ferrotoroidic ordering and is described as a phenomenon that the electromagnetic absorption spectrum depends on the direction of the wave vector of the incident light relative to the toroidal moment $\vec{T}$ (or $\vec{P}\times\vec{M}$; see discussions in Section 2.2) [97]. However, Di Matteo et al. [98] have shown that NDD has contributions from a magnetic quadrupole, a toroidal polar moment and magnetic octupole moments, in contrast to the natural circular dichroism, which is a measure of only the axial toroidal quadrupole moment of a system.

Another mechanism of observation by optical effects is based on the space-time symmetry of the second-order nonlinear susceptibility of materials with toroidal ordering. The second-harmonic generation (SHG) effect has been exploited to image the ferrotoroidic domain in $LiCoPO_4$ [53, 78]. An incident light impinges the crystal and induces emission of electromagnetic waves from it, including the SHG wave. The nonlinear optical response of the crystal is determined by the crystal symmetry and microscopic structure. In addition, the long-range ordering and other additional order parameters affect the symmetry in different ways. Therefore, the SHG in general is differently polarized by different ordering parameters. As an example, the ferrotoroidic domains caused by different toroidal ordering T_z and T_y in a $LiCoPO_4$ (100) sample was imaged with SHG light at 2.197 eV [53, 78] (see Figure 3B).

3.3 Dynamic toroidal moments in artificial metamolecules and dielectric nanostructures

In addition to static toroidal moments in various condensed materials, engineered toroidal moments using the concepts in plasmonic and metamaterials [99] cause growing interest, as such moments can be excited by and interact with electromagnetic fields more efficiently than the toroidal moments in condensed matter [100]. This helps us to understand the basis of dynamic toroidal

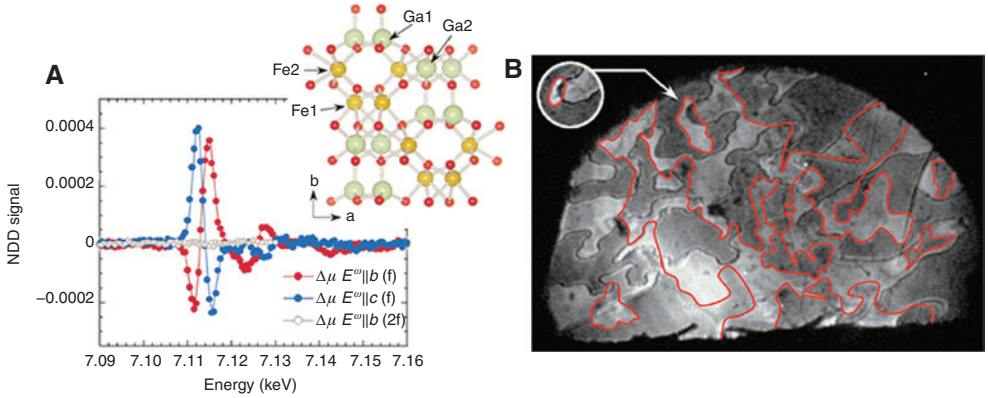

Figure 3: Examples of the interaction between optical waves and toroidal materials.
(A) NDD signal measured from a $GaFeO_3$ crystal for a polarization of the incident X-rays being aligned as $E^\omega \parallel b$ and $E^\omega \parallel c$, where a and b are depicted in the inset [96]. (B) Ferrotoroidic domains of a $LiCoPO_4$ (100) sample at 10 K imaged with SHG light at 2.197 eV [78]. Black and red lines indicate the different ferrotoroidic domain walls caused by T_z and T_y, respectively. Inset: ferrotoroidic domain movement caused by a temperature cycle. Figures reprinted with permission from (A) Ref. [96], APS; (B) Ref. [78], NPG.

moments interacting with light as well as modifying the optical properties of materials.

However, the toroidal dipole response in electrodynamics is often masked by more dominant electric and magnetic multipoles at similar energies. Therefore, artificial toroidal metamaterials are initially designed to amplify toroidal moments and suppress the competing electric and magnetic multipoles. This interesting field was set off by mimicking toroidal coils [52, 100] at microwave frequency to explore the toroidal dipole response in a great variety of structures as well as entering the optical regime by scaling structures down to the nanoscale [57]. Figure 4 gives a brief but not complete overview of different investigated toroidal metamolecules in catalogues of split-ring resonators and their variants, magnetic resonators, apertures, plasmonic cavities and structures, and dielectric nanostructures. It should be mentioned that the classification of metamaterials is not restricted to a single catalogue, for example, metallic double disks can be either considered as magnetic resonators [106, 117] or plasmonic cavities [118]. There are also other novel designs, for example, vertically assembled dumbbell-shaped apertures and split ring resonators resulting in a horizontal toroidal response in the optical region [119, 120].

The far-field radiation patterns of a toroidal moment are virtually identical with those of dipolar electric and magnetic moments, even though these moments are fundamentally different [24, 55] (see Section 3.4). The destructive interference between their radiation patterns has been exploited to construct a nonradiating scatterer. This approach is called the anapole excitation [104], scattering transparency [114], or analogous electromagnetic-induced transparency [102]. Such an intriguing design has promising potential applications in designing low-loss, high-quality factor cavities for sensing, lasers, qubits, and nonscattering objects for cloaking behavior. The anapole configuration is described in detail in Section 5.1.

In parallel, the dielectric metamaterial [121] was proposed to overcome dissipation loss of metals as encountered in metal-based toroidal metamaterial [112]. It has been pointed out that dissipation losses in metals originating from the ohmic resistance can hinder the excitation of toroidal multipoles, especially in the optical regime, resulting in weak coupling to external fields.

A fantastic characteristic of toroidal metamaterials as aforementioned is the feasibility in tuning toroidal responses via size, shape, material [114], and spatial arrangement and symmetry [56] of the constitutive elements [122]. So far, the major existing toroidal metamolecules are designed to achieve pronounced magnetic toroidal dipole response due to their peculiar property of asymmetry in both spatial inversion and time reversal. In this case, introducing space-inversion asymmetry, from either the geometry or the excitation source, is necessary for toroidal moment excitation, while breaking time-reversal symmetry has already been fulfilled by the magnetic dipole intrinsically. These toroidal artificial structures open an avenue to study the interaction with electromagnetic radiation in both the far-field and the near-field.

3.4 Electromagnetic fields and radiation patterns associated with toroidal moments

The electromagnetic field of a toroidal dipole can be suitably derived by using the retarded Green's function [65, 123, 124]. Considering an infinitesimal toroidal moment with arbitrary orientation as $\vec{T}$ oscillating at the angular frequency ω, the time-harmonic field components at the position $\vec{r} = R\hat{n}$ is given by

$$\begin{aligned}\vec{E}(\vec{r},\,t) &= \left\{-\frac{i\omega}{c}\frac{3(\vec{T}\cdot\hat{n})\hat{n}-\vec{T}}{R^3}+\frac{\omega^2}{c^2}\frac{3(\vec{T}\cdot\hat{n})\hat{n}-\vec{T}}{R^2}+\frac{i\omega^3}{c^3}\frac{\hat{n}\times(\hat{n}\times\vec{T})}{R}\right\}\exp(-i\omega t+kR)+c.c.\\ \vec{B}(\vec{r},\,t) &= \left\{-\frac{\omega^2}{c^2}\frac{\vec{T}\times\hat{n}}{R^2}-i\frac{\omega^3}{c^3}\frac{\vec{T}\times\hat{n}}{R}\right\}\exp(-i\omega t+kR)+c.c.\end{aligned} \tag{3}$$

The vector-field profile around the toroidal moment has also a toroidal configuration, as shown in Figure 5A. Interestingly, the electric field component of an oscillating toroidal dipole has three components depending on R^{-3}, R^{-2} and R^{-1}, respectively, dissimilar to the electric and magnetic dipoles, which depend on R^{-3} only. This fact has consequences on the interaction between toroidal dipoles and other classes of dipoles, as the interferences between the different parts causes the cancellation of free energy at specific distance-frequencies, at which the free energy becomes equal to zero. The interaction between two toroidal moments $\vec{T}_1$ and $\vec{T}_2$ in free space is given by $H^{\text{int}} \propto \omega \text{Re}\{-i\vec{T}_2 \cdot \vec{E}_1^{\star}(\omega, R_2)\}$. Using Eq. (3), the interaction energy is calculated as

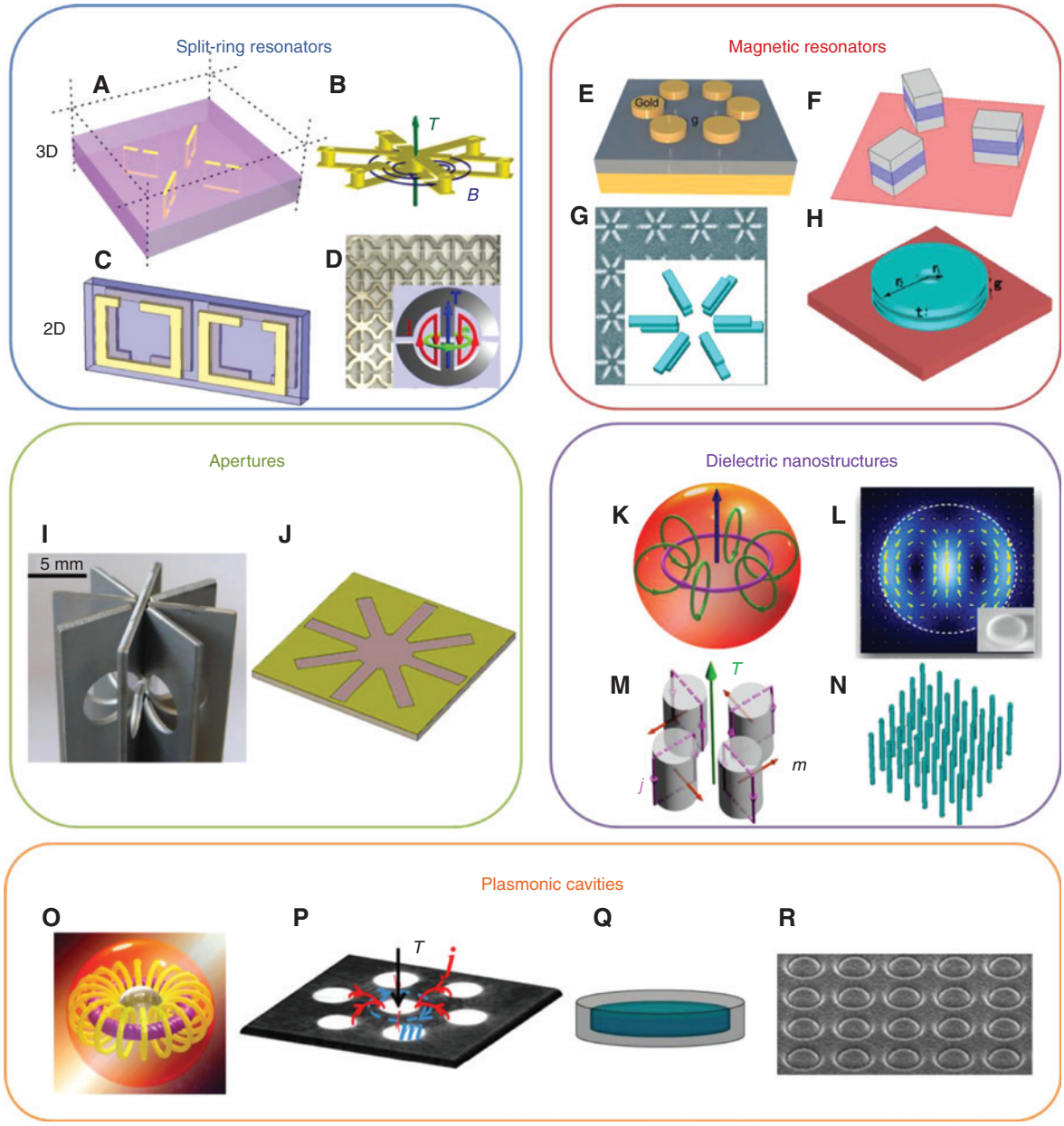

Figure 4: A brief overview of the investigated metamolecules with toroidal dipolar responses.
Split-ring resonators (SRR): (A) Schematic drawing of 3D SRR constituted by four rectangular metallic wire loops embedded in a dielectric slab [101]. (B) A combined SRR by sharing a central connecting bridge [102]. (C) An asymmetric SRR-based planar toroidal metamaterial [103]. (D) Planar conductive metamaterials formed by two symmetrical split rings [104]. Magnetic resonators: (E) an optical toroidal structure composed of a gold hexamer and metallic mirror separated by a dielectric layer [105]. (F) Three magnetic resonators consisting of two metallic rods and a dielectric spacer [106]. (G) An infrared toroid metamaterial composed of asymmetric double bars [107]. (H) A THz flat-ring-dimer (metallic double disks) toroidal metamaterial [108]. Apertures: (I) Toroidal metamaterial arrays consisting of dumbbell-shaped apertures manifest the destructive interference between electric and toroidal dipole moments leading to scattering transparency [54]. (J) Electric toroidal dipolar response has been achieved by metamaterial based on sun-like aperture element at microwave frequency [109]. Dielectric nanostructures: (K) Dielectric nanoparticle [110]. (L) Dielectric nanodisk with illustration of toroidal electric field distribution [111]. (M) Dielectric cylinders [112]. (N) Dielectric nanotubes [113]. Plasmonic cavities: (O) Core-shell nanoparticles support toroidal dipole excitation by a plan wave [114]. (P) Plasmonic oligomer nanocavities with seven nanoholes in metallic films sustain toroidal responses at visible wavelengths [19]. (Q) Toroidal modes are sustainable in the infrared and visible regime by sidewall-coated plasmonic nanodisk antenna [115]. (R) Circular V-groove array supports plasmon toroidal mode at optical frequencies [116]. Figures reprinted with permission from (A) Ref. [101], APS; (B) Ref. [102], Wiley-VCH Verlag GmbH & Co. KGaA, Weinheim; (C) Ref. [103], APS; (D) Ref. [104], APS; (E) Ref. [105], NPG; (F) Ref. [106], by courtesy of Jing Chen; (G) Ref. [107], AIP; (H) Ref. [108], Elsevier B.V.; (I) Ref. [54], NPG; (J) Ref. [109], AIP; (K) Ref. [110], OSA; (L) Ref. [111], NPG; (M) Ref. [112], APS; (N) Ref. [113], OSA; (O) Ref. [114], Wiley-VCH Verlag GmbH & Co. KGaA, Weinheim; (P) Ref. [19], AIP; (Q) Ref. [115], ACS; (R) Ref. [116], OSA.

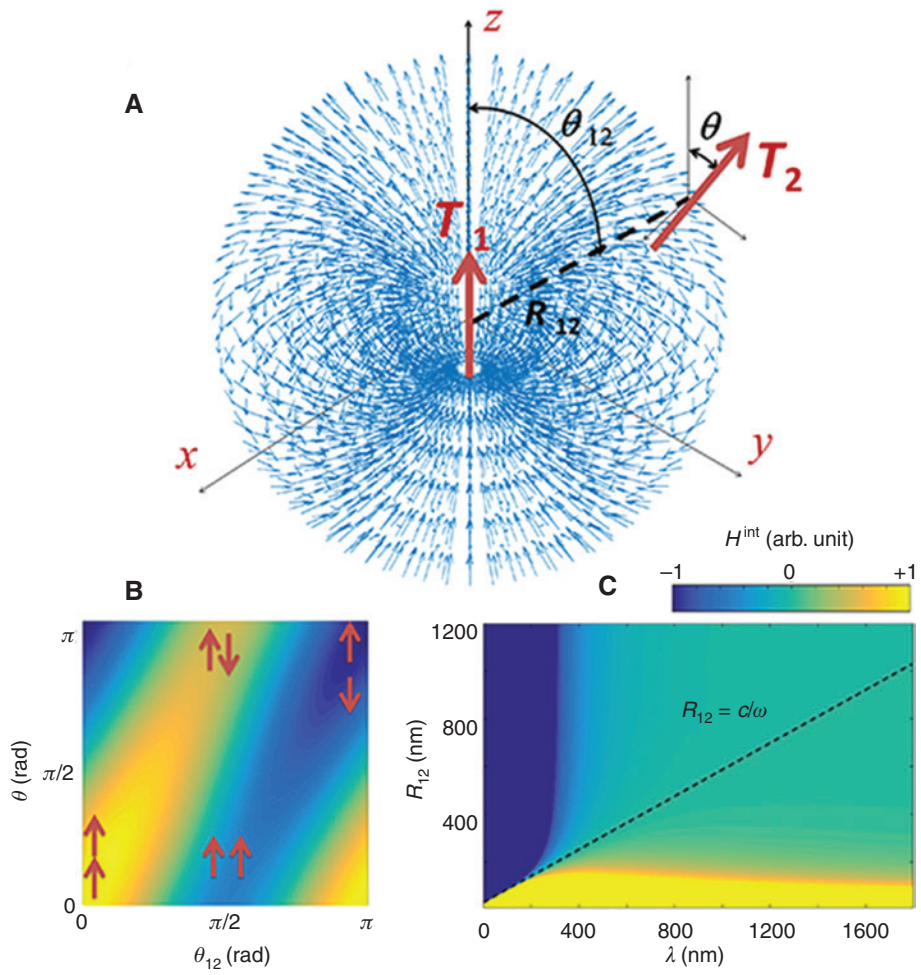

Figure 5: Toroidal field profile and the interaction energy between two toroidal dipoles.
(A) Electric-field configuration associated with a toroidal dipole moment positioned at the origin of the coordinate system. Another toroidal dipole moment positioned at the proximity of the original toroidal dipole moment can couple with it. (B) The interaction energy of two coupled toroidal moments versus the polar angles θ_{12} and θ and (C) versus the wavelength and the distance between them. Positive and negative interaction energies produce the higher- and lower-energy states in a hybridization picture, respectively. The arrows show the orientation of toroidal moments. The color bar is identical for (B) and (C).

$$H^{\text{int}} = -(3(\vec{T}_1\cdot\hat{n})(\vec{T}_2\cdot\hat{n}) - \vec{T}_1\cdot\vec{T}_2)\left[\left(\frac{\omega}{c}\right)\frac{1}{R_{12}^3} - \left(\frac{\omega}{c}\right)^3\frac{1}{R_{12}}\right], \qquad (4)$$

in which it is assumed that both multipoles oscillate at the same frequency and R_{12} is the distance between two multipoles. The interaction energy between two multipoles oriented as $\vec{T}_1 = T_1\hat{z}$ and $\vec{T}_2 = T_2\cos(\theta)\hat{z} + T_2\sin(\theta)\hat{x}$ positioned at a distance $R_{12} < c/\omega$ versus the polar angles θ_{12} and θ is shown in Figure 5. In a hybridization picture, a negative interaction energy between the moments produces the lower-energy state of a system of coupled toroidal moments, whereas a positive interaction energy causes the higher-energy state. The interaction energy between two toroidal dipoles sustains an extremum at configurations depicted in Figure 5B; i.e. when the two toroidal dipoles are oriented either parallel or antiparallel in a transverse or longitudinal arrangement. This is very similar to the coupling between two electric dipoles [125]. Dissimilar to the case of coupled electric dipoles, however, the interaction energy between two toroidal dipoles can be quite different at distances $R_{12} < c/\omega$ and $R_{12} > c/\omega$, even for a fixed arrangement and orientation of toroidal dipoles. It is already obvious from Eq. (4) that at $R_{12} = c/\omega$, $H^{\text{int}} = 0$ (see Figure 5C). This fact causes switching of the eigenenergies for symmetric and antisymmetric coupling at distances ranging from $R_{12} < c/\omega$ to $R_{12} > c/\omega$. It should also be mentioned that for localized toroidal moments this, switching might not be an obvious fact, as the critical distance $R_{12} = c/\omega$ is comparable to the wavelength,

which is usually much larger than the scale of a toroidal dipole moment source. For a nonlocalized metamaterial-based toroidal moment coupling configuration which is comparable to the scale of the wavelength, this switching becomes better observable.

The radiation pattern associated to a toroidal dipole moment is given by $P=(c/4\pi)R^2\hat{n}\cdot\mathrm{Re}\{\vec{E}(\vec{r},t)\times\vec{B}^*(\vec{r},t)\}$, which, after some simple algebraic manipulations, is simplified to $(\omega^6/4\pi c^5)(|\vec{T}|^2-(\hat{n}\cdot\vec{T})^2)$. This is quite similar to the radiation pattern of an electric dipole moment [24]. Particularly, they share the same multipolarity and angular radiation pattern and show different frequency dependencies. This holds for the higher-order multipoles too and is very important when they coexist and compete. Interestingly, different contributions to the near-field profile of the toroidal moment cancel themselves in the far-field pattern, and only the last term in Eq. (3) contributes to the radiation pattern.

4 Excitation of toroidal moments

4.1 External light

Whereas the detection of natural spin-based toroidal moments of solid states needs complicated methods like X-ray gyrotropy and circular dichroism [98, 126], X-ray Compton scattering [127], nonreciprocal reflection [128], or second harmonic generation [53], the excitation and detection of dynamic metamaterial-based toroidal moments are apparently much simpler. This is because each element of the metamaterial configuration is designed in an intelligent way to (i) couple effectively with the incident light and (ii) sustain an effective ring-like orientation of magnetic moments as shown in Figure 1C, which can be arranged in arbitrary numbers of magnetic moments in the ring affecting directly the strength of toroidal moments.

Depending on the polarity of light and the spatial symmetry of the metamaterial structures, different strategies are used to excite toroidal moments in metamaterials. In the literature, external light, with either linear [129], radial [105, 130], or circular polarization [101, 109], has been used to illuminate the metamaterials normally, laterally, or obliquely (see Figure 6).

In general, the polarization of the electric field of the incident light induces effective current loops in the structure, which generates magnetic dipoles. By carefully arranging the structure elements and the polarization direction of the incident light, a vortex of magnetic dipoles, i.e. a toroidal moment, is thus achieved. For instance, split-ring resonators usually are illuminated from a lateral direction.

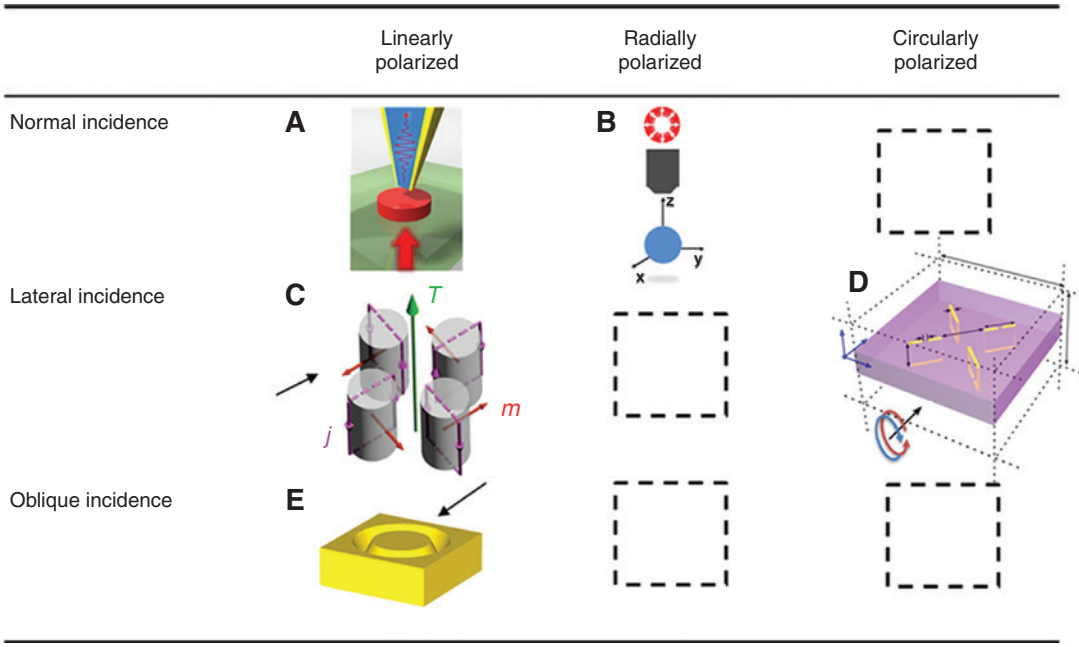

Figure 6: Different excitation strategies for toroidal moments in metamaterials via polarization and incidence directions. Dashed boxes denote no published result yet. Figure reproduced from (A) Ref. [111], Creative Commons CC-BY license; (B) Ref. [130], OSA; (C) Ref. [112], APS; (D) Ref. [101], APS; (E) Ref. [116], OSA.

4.2 Relativistic electrons

Relativistic electrons possess a unique spatial structure of the electromagnetic field attached to their vicinity. Distinct to far-field light sources, relativistic electrons act not only as a near-field excitation source, but also share certain overlapping excitation features with various optical excitation field geometries in an ultra-broad band frequency range, such as a radial and circular far-field [131], and a dipolar near-field (Figure 7) [19, 132]. Such combined electronic and optical excitations allow a comprehensive study of toroidal metamaterials.

Recently, electron energy loss spectroscopy (EELS) and energy-filtered transmission electron microscopy (EFTEM) with relativistic electrons have been used to study toroidal moments at high spatial resolution [132]. EELS and EFTEM use focused and parallel electron beams, respectively, which can interact with the optical modes of the sample. Due to this inelastic interaction, the electron loses energy, which can be detected using an electron spectrometer. The energy loss suffered by the electron is an indirect probe of the optical resonances of the sample [133–137].

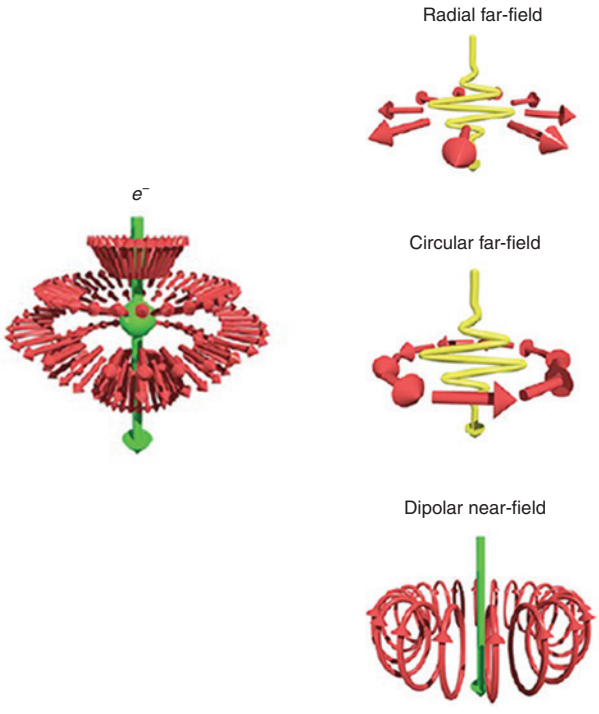

Figure 7: Electromagnetic-field components surrounding a relativistic electron. The excitation of relativistic electrons shares certain symmetric features with that of a radial and circular far-field, and of a dipolar near-field. Reprinted with permission from Ref. [132]. Copyright (2012) American Chemical Society.

5 Coupling of toroidal moments to other classes of moments

5.1 Formation and discovery of anapoles

Nonradiating field distributions and sources have attracted attention from time to time, mainly due to their connection with the discovery and characterization of elementary charged particles. A very prominent example of such a category is an electron, with the well-known Coulomb field associated with it, which even at a uniform velocity maintains its evanescent field profile. Classically, several current distributions were heuristically introduced with vanishing far-field radiation. An interesting work in this field, initiated by Devaney and Wolf [138], has considered the multipole expansion of the fields generated by time-harmonic current distributions inside an enclosed region specified by $r<R$, to conclude that the radiation multipole moments are dependent only on the transverse components of the spatial-harmonic current density distribution given by $\tilde{\vec{J}}^T(K,\omega)=(\vec{K}\times\tilde{\vec{J}}(\vec{K},\omega))\times\vec{K}/K^2$. This statement is valid only for those components for which $\vec{K}=k_0=\omega/c$ [138]. In other words, a nonradiating source should have a vanishing $\tilde{\vec{J}}^T(K=k_0,\omega)$ component [138–140]. However, the classification of multipole moments as provided by Devaney and Wolf excludes the toroidal moment class. For including toroidal moments, a complete analysis as discussed above is necessary.

An example of a nonradiating source is known as an anapole. An anapole is composed of a toroidal dipole moment and an electric dipole moment. As the radiation pattern associated to these two classes of moments are quite similar to each other, even in the near-field (see discussions in Section 3.4), it is possible to precisely tune the strength of these two moments by means of geometry [111, 141] (Figure 8A and B), in order to cancel the radiation pattern, even though the field components of a toroidal dipole moment being proportional to R^{-2} and R^{-3} will still contribute to the near-field profile. In fact, the anapole moment was first introduced theoretically by Zeldovich [142]. For quite a long time, however, discussions regarding the existence of such a moment were just theoretical. The first experimental evidence for the existence of an anapole in the cesium atomic nuclei has been published in 1997 by Wood et al. [143]. Among the applications of the anapole moment are its relation to dark matter in the universe [144, 145], enhancing light absorption by metamolecules with an anapole moment [146], and enhancing efficiency of higher harmonics generation [141], have been already discussed in the literature.

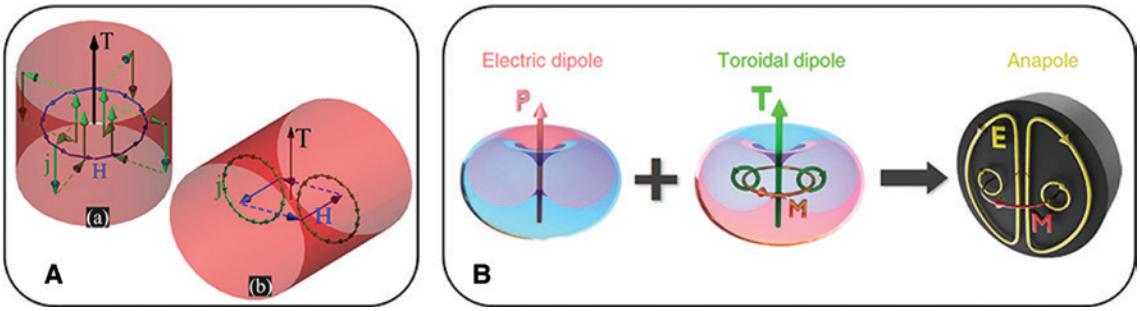

Figure 8: The combination of a magnetic toroidal dipole moment and an electric dipole moment in a dielectric (A) nanorod [141] and (B) nanodisc can create an anapole moment [111]. Figure reproduced from (A) Ref. [141], OSA; (B) Ref. [111], Creative Commons CC-BY license.

5.2 Toroidal metamaterials

Despite the fact that different configurations of toroidal metamolecules have been so far intensively investigated for their intriguing possibilities to sustain toroidal moments, still the coupling between adjacent elements have not been thoroughly studied yet. In fact, due to the exotic near-field contribution, such a coupling and hybridization of toroidal moment can obey quite different selection rules in comparison with electric and magnetic dipoles. Moreover, even neglecting the coupling between adjacent elements, an arrangement of toroidal moments in a photonic crystal lattice leads to interesting new behaviors such as resonant transparency and Fano excitations within the effective-medium approximation [52, 54, 102].

6 Applications of toroidal moments

The formation of toroidal moments in a spatially confined hybrid electric-magnetic configuration leads to unusual properties, which opens a horizon of potential applications in data storing [147] and designing of low-loss metamaterials or metadevices [129, 148–150], such as ultrasensitive sensors and diagnostic tools [101, 151], polarization twister [109], near-field lasing [152] and lasing spacer [153].

For long-range toroidal moments in condensed-matter systems, their inherent ME is of technological interest since it provides an alternative and convenient way for manipulation of data in for example storage discs. Indeed, data storing at the nanoscale can be realized by switchable, ordered electric toroidal moments in low-dimensional ferroelectric structures [147, 154]. Moreover, the switching of toroidal moments requires no electrode contact at the nanoscale but is conveniently controlled by time-dependent magnetic fields. Additionally, it exhibits no noticeable cross-talk [154]. As for the case of $LiCoPO_4$, the generation and manipulation of ferrotoroidic domains were implemented by simultaneously applied magnetic and electric fields, not solely by either of the fields alone [53]. It gives the material a promising potential to reject external disturbance in data storage, as an illustration. Moreover, the intrinsic linear ME of ferrotoroidic materials is anticipated to be a source of giant MEs via effective enhancement [87].

Benefiting from more confinement in real space, dynamic toroidal dipolar excitation in metamaterials usually achieves higher quality factors by carefully designing the geometry [129, 148, 149] and the chemical component [152]. It paves the road for applications as low-loss, high-Q cavities in metadevices [103, 104, 148–150] and laser spacer [153]. Through destructive or constructive interference between toroidal multipoles and electric or magnetic multipoles, astonishing electromagnetic phenomena can be achieved, such as manipulation from non- to super-radiating [130, 155], resonant transparency [54, 114, 156], extremely high Q-factors [104] and nanolasering in the near-field [152].

Instead of local toroidal excitations, a propagating toroidal excitation in free space, as a peculiar form of delivering an electromagnetic field, is intriguing. This concept was introduced in 1996 as focused doughnuts, a single-cycle, broad-bandwidth pulse with a spatially localized toroidal field configuration and longitudinal field components [157]. It was numerically shown that such pulses allow to excite a prominent toroidal dipole mode in a dielectric nanosphere [158]. The challenge of realizing such a focused doughnut lies in simultaneously controlling frequency and spatial dispersion over a wide bandwidth [24].

Another peculiar feature of toroidal moments is circular dichroism [101, 151]. It is seemingly challenging the common interpretation based on electric and magnetic quadrupoles and also might have a potential in diagnosing and sensing fields [101]. Moreover, an effective

conversion between left-handed to right-handed circularly polarized waves at the same frequency has been demonstrated via arrays of sun shape apertures [109]. It can be potentially applied as polarization twister at the microwave region.

7 Conclusion and outlook

The basis of toroidal moments based on a multipole expansion of the vector potential and expansion of the free energy is reexamined. Static toroidal moments widely exist in condensed matter, and dynamic toroidal moments have become unambiguous via metamaterial engineering in the last few years. The peculiar behavior of toroidal moments is determined by their hybrid nature in a charge-current configuration. Investigation of the associated characteristics and potential applications of toroidal moments has started up and drawn increasing attention. Nevertheless, many unknown aspects and concepts still wait for exploration and inspection. We mention a few possible future directions in the following.

The intrinsic ME associated to toroidization in condensed matter has possible technological applications in data storage, where faster switching and more controllability are anticipated via the concomitant utilization of the static electric and magnetic fields. Obviously, data bits in such a device are written and read via the ME. However, still, the effect should be enhanced prior to the employment in technologically relevant storage devices.

A promising toroidal element in solid state systems is the skyrmion. It is the smallest possible perturbation to a uniform magnet, displaying as a localized solitonic magnetic whirls (spins) usually with a width of a few tens of atoms [159, 160]. Skyrmion-based devices are anticipated to store and process information at unprecedentedly small sizes and levels of energy consumption [160].

Considering electrodynamics, aside from designing metamolecules with prominent toroidal dipole response, the radiation properties associated to toroidal moments and the interaction between toroidal moments require more attention. In particular, coupling between the toroidal moments and their associated collective excitations is to be experimentally investigated, to enable engineering systems based on toroidal moments. Moreover, due to similarities between the Helmholtz and Schrödinger equations, it is of paramount interest to investigate the coupling of toroidal metamolecules to the applied probes, such as matter waves and light. The size of the supported metamolecules is often at the nanoscale, especially when toroidal responses enter the optical regime. Thus, the state-of-the-art microscopy techniques are helpful to generate and observe toroidal fields at the nanoscale, such as electron energy-loss spectroscopy, cathodoluminescence, scanning tunneling microscopy, and scanning near-field optical microscopy.

Observation of toroidal modes in dielectric and metallic photonic crystals can endeavor new engineering routes of the optical density of states, beyond what is to be expected from the dipole approximation. Inclusion of toroidal moments, especially toroidal cavities with high-quality factors, has a high potential for engineering the Purcell factor due to its deep-subwavelength mode volume [118]. More interestingly, photonic crystals and toroidal cavities designed in a precise way for quenching the radiation from dyes can provide a new path for nonradiative energy transfer between the adjacent elements, by incorporating the concept of anapoles. Additionally, we anticipate that the coupling of the whispering gallery modes of tapers and fibers [27, 161] to the axial toroidal moments at the apex of a SNOM tip will be an interesting option to introduce new near-field microscopes with higher efficiencies and long-range coupling probabilities compared to the generally used SNOM tips, which are based on dipole-dipole interactions. Such a configuration might be used to probe the magnetic field, in a competing configuration with well-known spin-coded SNOM tips [72].

Acknowledgment: S.G. thanks Max-Planck-Society for a Ph.D. scholarship. Authors gratefully acknowledge Wilfried Sigle for constructive and fruitful discussions.

References

[1] A year to remember. Nat Photon 2015:9:1.
[2] Diener G. Superluminal group velocities and information transfer. Phys Lett A 1996;223:327–31.
[3] Chen P, Shu C, Guo XX, Loy MMT, Du SW. Measuring the biphoton temporal wave function with polarization-dependent and time-resolved two-photon interference. Phys Rev Lett 2015;114:010401.
[4] Yamamoto T, Yamashita S, Yajima S. Wave function of a photon and the appropriate Lagrangian. J Phys Soc Jpn 2012;81:024402.
[5] Bialynickabirula Z, Bialynickibirula I. Reconstruction of the wave-function from the photon number and quantum phase distributions. J Mod Optic 1994;41:2203–8.
[6] Pendry JB, Schurig JB, Smith DR. Controlling electromagnetic fields. Science 2006;312:1780–2.
[7] Shalaev VM, Cai WS, Chettiar UK, et al. Negative index of refraction in optical metamaterials. Opt Lett 2005;30:3356–8.
[8] Vakil A, Engheta N. Transformation optics using graphene. Science 2011;332:1291–4.

[9] Luk'yanchuk B, Zheludev NI, Maier SA, et al. The Fano resonance in plasmonic nanostructures and metamaterials. Nat Mater 2010;9:707–15.
[10] Talebi N, Shahabdi M. Analysis of the propagation of light along an array of nanorods using the generalized multipole techniques. J Comput Theor Nanos 2008;5:711–6.
[11] Talebi N, Shahabadi M. Spoof surface plasmons propagating along a periodically corrugated coaxial waveguide. J Phys D Appl Phys 2010;43:135302.
[12] Leonhardt U. Optics – momentum in an uncertain light. Nature 2006;444:823–4.
[13] Kemp BA. Resolution of the Abraham-Minkowski debate: implications for the electromagnetic wave theory of light in matter. J Appl Phys 2011;109:111101.
[14] Zhou F, Li ZY, Liu Y, Xia YN. Quantitative analysis of dipole and quadrupole excitation in the surface plasmon resonance of metal nanoparticles. J Phys Chem C 2008;112:20233–40.
[15] Talebi N, Shahabadi M, Khunsin W, Vogelgesang R. Plasmonic grating as a nonlinear converter-coupler. Opt Express 2012;20:1392–405.
[16] Willingham B, Link S. Energy transport in metal nanoparticle chains via sub-radiant plasmon modes. Opt Express 2011;19:6450–61.
[17] Maier SA, Kik PG, Atwater HA, et al. Local detection of electromagnetic energy transport below the diffraction limit in metal nanoparticle plasmon waveguides. Nat Mater 2003;2:229–32.
[18] Bajestani SMRZ, Shahabadi M, Talebi N. Analysis of plasmon propagation along a chain of metal nanospheres using the generalized multipole technique. J Opt Soc Am B 2011;28:937–43.
[19] Talebi N, Ögüt B, Sigle W, Vogelgesang R, Van Aken PA. On the symmetry and topology of plasmonic eigenmodes in heptamer and hexamer nanocavities. Appl Phys A 2014;116:947–54.
[20] Talebi N, Mahjoubfar A, Shahabadi M. Plasmonic ring resonator. J Opt Soc Am B 2008;25:2116–22.
[21] Zeldovich IB. Electromagnetic interaction with parity violation. Sov Phys Jetp-Ussr 1958;6:1184–6.
[22] Dubovik VM, Tugushev VV. Toroid moments in electrodynamics and solid-state physics. Phys Rep 1990;187:145–202.
[23] Spaldin NA, Fiebig M, Mostovoy M. The toroidal moment in condensed-matter physics and its relation to the magnetoelectric effect. J Phys Condens Matter 2008;20:434203.
[24] Papasimakis N, Fedotov VA, Savinov V, Raybould TA, Zheludev NI. Electromagnetic toroidal excitations in matter and free space. Nat Mater 2016;15:263–71.
[25] Elschner J, Hu GH. Scattering of plane elastic waves by three-dimensional diffraction gratings. Math Mod Meth Appl S 2012;22:1150019.
[26] Gallagher DFG, Felici TP. Eigenmode expansion methods for simulation of optical propagation in photonics – pros and cons. Proc SPIE 2003;4987:69–82.
[27] Talebi N, Sigle W, Vogelgesang R, et al. Excitation of mesoscopic plasmonic tapers by relativistic electrons: phase matching versus eigenmode resonances. ACS Nano 2015;9:7641–8.
[28] Raab RE, De Lange OL. Multipole theory in electromagnetism: classical, quantum, and symmetry aspects, with applications. New York, Oxford, Oxford University Press, 2005.
[29] Vrejoiu C. Electromagnetic multipoles in Cartesian coordinates. J Phys A-Math Gen 2002;35:9911–22.
[30] Harrington RF. Time-harmonic electromagnetic field. New York, Toronto, London, McGraw-Hill Book Company, 1961.
[31] Gray CG. Multipole expansions of electromagnetic-fields using Debye potentials. Am J Phys 1978;46:169–79.
[32] Jackson JD. Classical electrodynamics, 3rd ed. New York, John Wiley & Sons, Inc., 1999.
[33] Pershan PS. Nonlinear optical properties of solids: energy considerations. Phys Rev 1963;130:919–29.
[34] Balandin AL. The method of multipole fields for 3D vector tomography. Comput Appl Math 2016;35:203–18.
[35] Agarwal K, Chen XD, Zhong Y. A multipole-expansion based linear sampling method for solving inverse scattering problems. Opt Express 2010;18:6366–81.
[36] Potthast R. A point source method for inverse acoustic and electromagnetic obstacle scattering problems. IMA J Appl Math 1998;61:119–40.
[37] Jerbi K, Mosher JC, Baillet S, Leahy RM. On MEG forward modelling using multipolar expansions. Phys Med Biol 2002;47:523–55.
[38] Kyurkchan AG. On the method of auxiliary currents and sources for the diffraction wave problems. Radiotekh Elektron 1984;29:2129–39.
[39] Shubitidze F, O'neill K, Haider SA, Sun K, Paulsen KD. Application of the method of auxiliary sources to the wide-band electromagnetic induction problem. IEEE Trans Geosci Remote Sens 2002;40:928–42.
[40] Kaklamani DI, Anastassiu HT. Aspects of the method of auxiliary sources (MAS) in computational electromagnetics. IEEE Antennas Propag Mag 2002;44:48–64.
[41] Hafner C, Ballisti R. The multiple multipole method (MMP). COMPEL 1983;2:1–7.
[42] Hafner C, Klaus G. Application of the multiple multipole (MMP) method to electrodynamics. COMPEL 1985;4:137–44.
[43] Moreno E, Erni D, Hafner C. Band structure computations of metallic photonic crystals with the multiple multipole method. Phys Rev B 2002;65:155120.
[44] Talebi N, Shahabadi M, Hafner C. Analysis of a lossy microring using the generalized multipole technique. Prog Electromagn Res 2006;66:287–99.
[45] Ludwig AC. The generalized multipole technique. Comput Phys Commun 1991;68:306–14.
[46] Raeis-Zadeh SM, Safavi-Naeini S. Analysis of electromagnetic wave scattering by graphene flakes using the generalized multipole technique. IEEE Trans Antennas Propag 2016;64:1032–8.
[47] Landesa L, Obelleiro F, Rodriguez JL. Inverse scattering of impenetrable objects using the generalized multipole technique. Microw Opt Techn Let 1998;18:429–32.
[48] Talebi N, Shahabadi M. Application of generalized multipole technique to the analysis of discontinuities in substrate integrated waveguides. PIER 2007;69:227–35.
[49] Talebi N, Shahabadi M. All-optical wavelength converter based on a heterogeneously integrated GaP on a silicon-on-insulator waveguide. J Opt Soc Am B 2010;27:2273–8.
[50] Hafner C. The multiple multipole program (MMP) and the generalized multipole technique (GMT) A2 – Wriedt, Thomas, in generalized multipole techniques for electromagnetic and light scattering. Amsterdam, Elsevier Science B.V., 1999, 21–38.
[51] Dubovik V, Tosunyan L, Tugushev V. Axial toroidal moments in electrodynamics and solid-state physics. Zh EkspTeor Fiz 1986;90:590–605.

[52] Marinov K, Boardman AD, Fedotov VA, Zheludev N. Toroidal metamaterial. New J Phys 2007;9:324.
[53] Zimmermann AS, Meier D, Fiebig M. Ferroic nature of magnetic toroidal order. Nat Commun 2014;5:4796.
[54] Fedotov VA, Rogacheva AV, Savinov V, Tsai DP, Zheludev NI. Resonant transparency and non-trivial non-radiating excitations in toroidal metamaterials. Sci Rep 2013;3:2967.
[55] Savinov V, Fedotov VA, Zheludev NI. Toroidal dipolar excitation and macroscopic electromagnetic properties of metamaterials. Phys Rev B 2014;89:205112.
[56] Kaelberer T, Fedotov VA, Papasimakis N, Tsai DP, Zheludev NI. Toroidal dipolar response in a metamaterial. Science 2010;330:1510–2.
[57] Huang Y-W, Chen WT, Wu PC, et al. Design of plasmonic toroidal metamaterials at optical frequencies. Opt Express 2012;20:1760–8.
[58] Thorner G, Kiat J-M, Bogicevic C, Kornev I. Axial hypertoroidal moment in a ferroelectric nanotorus: a way to switch local polarization. Phys Rev B 2014;89:220103.
[59] Talebi N. Optical modes in slab waveguides with magnetoelectric effect. J Opt 2016;18:055607.
[60] Jackson JD. From Lorenz to Coulomb and other explicit gauge transformations. Am J Phys 2002;70:917–28.
[61] Góngora TA, Ley-Koo E. Complete electromagnetic multipole expansion including toroidal moments. Rev Mex Fis E 2006;52:188–97.
[62] Spaldin NA, Fechner M, Bousquet E, Balatsky A, Nordström L. Monopole-based formalism for the diagonal magnetoelectric response. Phys Rev B 2013;88:094429.
[63] Preskill J. Magnetic monopoles. Annu Rev Nucl Part S 1984;34:461–530.
[64] Artamonov YA, Gorbatsevich AA. Symmetry and dynamics of systems with toroidal moments. Zh Eksp Teor Fiz 1985;89:1078–93.
[65] Radescu EE, Vaman G. Exact calculation of the angular momentum loss, recoil force, and radiation intensity for an arbitrary source in terms of electric, magnetic, and toroid multipoles. Phys Rev E Stat Nonlin Soft Matter Phys 2002;65:046609.
[66] Schwanecke AS, Fedotov VA, Khardikov VV, Prosvirnin SL, Chen Y, Zheludev NI. Nanostructured metal film with asymmetric optical transmission. Nano Lett 2008;8:2940–3.
[67] Nanz S. Toroidal multipole moments in classical electrodynamics. Wiesbaden, Springer, Spektrum, 2016.
[68] Sessoli R, Boulon M-E, Caneschi A, et al. Strong magneto-chiral dichroism in a paramagnetic molecular helix observed by hard X-rays. Nat Phys 2015;11:69–74.
[69] Lin SY, Wernsdorfer W, Ungur L, et al. Coupling Dy3 triangles to maximize the toroidal moment. Angew Chem Int Ed Engl 2012;51:12767–71.
[70] Li X-L, Wu J, Tang J, Le Guennic B, Shi W, Cheng P. A planar triangular Dy3 + Dy3 single-molecule magnet with a toroidal magnetic moment. Chem Commun 2016;52:9570–3.
[71] Chibotaru LF, Ungur L, Soncini A. The origin of nonmagnetic Kramers doublets in the ground state of dysprosium triangles: evidence for a toroidal magnetic moment. Angew Chem Int Ed Engl 2008;47:4126–9.
[72] Rondin L, Tetienne J-P, Spinicelli P, et al. Nanoscale magnetic field mapping with a single spin scanning probe magnetometer. Appl Phys Lett 2012;100:153118.
[73] Gusev A, Herchel R, Nemec I, et al. Tetranuclear lanthanide complexes containing a hydrazone-type ligand. Dysprosium [2 × 2] gridlike single-molecule magnet and toroic. Inorg Chem 2016;55:12470–6.
[74] Biswas S, Das S, Gupta T, et al. Observation of slow relaxation and single-molecule toroidal behavior in a family of butterfly-shaped Ln4 complexes. Chem Eur J 2016;22:18532–50.
[75] Scagnoli V, Staub U, Bodenthin Y, et al. Observation of orbital currents in CuO. Science 2011;332:696–8.
[76] Jodlauk S, Becker P, Mydosh JA, et al. Pyroxenes: a new class of multiferroics. J Phys 2007;19:432201.
[77] Popov YF, Kadomtseva AM, Vorob'ev GP, et al. Magnetoelectric effect and toroidal ordering in $Ga_{2-x}Fe_xO_3$. J Exp Theor Phys 1998;87:146–51.
[78] Van Aken BB, Rivera J-P, Schmid H, Fiebig M. Observation of ferrotoroidic domains. Nature 2007;449:702–5.
[79] Baum M, Schmalzl K, Steffens P, et al. Controlling toroidal moments by crossed electric and magnetic fields. Phys Rev B 2013;88:024414.
[80] Tolédano P, Ackermann M, Bohatý L, et al. Primary ferrotoroidicity in antiferromagnets. Phys Rev B 2015;92:094431.
[81] Yamaguchi Y, Kimura T. Magnetoelectric control of frozen state in a toroidal glass. Nat Commun 2013;4:2063.
[82] Ederer C, Spaldin NA. Towards a microscopic theory of toroidal moments in bulk periodic crystals. Phys Rev 2007;76:214404.
[83] Sannikov DG. Phenomenological theory of the magnetoelectric effect in some boracites. J Exp Theor Phys 1997;84:293–9.
[84] Sannikov DG, Schaack G. Theoretical temperature-electric-field phase diagram for betaine calcium chloride dihydrate. Phys Rev B 1998;58:8313–22.
[85] Sannikov DG. Ferrotoroic phase transition in boracites. Ferroelectrics 1998;219:177–81.
[86] Fiebig M, Meier D. From magnetic vortices to magnetic monopoles – ferrotoroidicity as fourth form of ferroic order. (Accessed April 4, 2017, at https://www.manep.ch/from-magnetic-vortices-to-magnetic-monopoles/.)
[87] Fiebig M, Lottermoser T, Meier D, Trassin M. The evolution of multiferroics. Nat Rev Mater 2016;1:16046.
[88] Popov YF, Kadomtseva AM, Belov DV, Vorob'ev GP, Zvezdin AK. Magnetic-field-induced toroidal moment in the magnetoelectric Cr_2O_3. J Exp Theor Phys 1999;69:330–5.
[89] Hehl FW, Obukhov YN, Rivera J-P, Schmid H. Relativistic nature of a magnetoelectric modulus of Cr_2O_3 crystals: a four-dimensional pseudoscalar and its measurement. Phys Rev 2008;77:022106.
[90] Wilczek F. Two applications of axion electrodynamics. Phys Rev Lett 1987;58:1799–802.
[91] Tellegen BDH. The gyrator, a new electric network element. Philips Res Rep 1948;3:81–101.
[92] Valencia S, Crassous A, Bocher L, et al. Interface-induced room-temperature multiferroicity in BaTiO(3). Nat Mater 2011;10:753–8.
[93] Yadav AK, Nelson CT, Hsu SL, et al. Observation of polar vortices in oxide superlattices. Nature 2016;530:198–201.
[94] Brown Jr WF, Shtrikman S, Treves D. Possibility of visual observation of antiferromagnetic domains. J Appl Phys 1963;34:1233–4.
[95] Hopfield JJ, Thomas DG. Photon momentum effects in the magneto-optics of excitons. Phys Rev Lett 1960;4:357–9.

[96] Kubota M, Arima T, Kaneko Y, He JP, Yu XZ, Tokura Y. X-ray directional dichroism of a polar ferrimagnet. Phys Rev Lett 2004;92:137401.
[97] Kibayashi S, Takahashi Y, Seki S, Tokura Y. Magnetochiral dichroism resonant with electromagnons in a helimagnet. Nat Commun 2014;5:4583.
[98] Di Matteo S, Joly Y, Natoli CR. Detection of electromagnetic multipoles by X-ray spectroscopies. Phys Rev B 2005;72:144406.
[99] Liu Y, Zhang X. Metamaterials: a new frontier of science and technology. Chem Soc Rev 2011;40:2494–507.
[100] Papasimakis N, Fedotov VA, Marinov K, Zheludev NI. Gyrotropy of a metamolecule: wire on a torus. Phys Rev Lett 2009;103:093901.
[101] Raybould TA, Fedotov VA, Papasimakis N, et al. Toroidal circular dichroism. Phys Rev B 2016;94:035119.
[102] Han S, Cong L, Gao F, Singh R, Yang H. Observation of Fano resonance and classical analog of electromagnetically induced transparency in toroidal metamaterials. Ann Phys 2016;528:352–7.
[103] Fan Y, Wei Z, Li H, Chen H, Soukoulis CM. Low-loss and high-Qplanar metamaterial with toroidal moment. Phys Rev B 2013;87:115417.
[104] Basharin AA, Chuguevsky V, Volsky N, Kafesaki M, Economou EN. Extremely high Q-factor metamaterials due to anapole excitation. Phys Rev B 2017;95:035104.
[105] Bao Y, Zhu X, Fang Z. Plasmonic toroidal dipolar response under radially polarized excitation. Sci Rep 2015;5:11793.
[106] Tang C, Chen J, Wang Q, et al. Toroidal dipolar response in metamaterials composed of metal-dielectric-metal sandwich magnetic resonators. EEE Photon J 2016;8:1–9.
[107] Dong Z-G, Zhu J, Rho J, et al. Optical toroidal dipolar response by an asymmetric double-bar metamaterial. Appl Phys Lett 2012;101:144105.
[108] Li J, Shao J, Li J-Q, et al. Optical responses of magnetic-vortex resonance in double-disk metamaterial variations. Phys Lett A 2014;378:1871–5.
[109] Guo L-Y, Li M-H, Huang X-J, Yang H-L. Electric toroidal metamaterial for resonant transparency and circular cross-polarization conversion. Appl Phys Lett 2014;105:033507.
[110] Liu W, Shi J, Lei B, Hu H, Miroshnichenko AE. Efficient excitation and tuning of toroidal dipoles within individual homogenous nanoparticles. Opt Express 2015;23:24738–47.
[111] Miroshnichenko AE, Evlyukhin AB, Yu YF, et al. Nonradiating anapole modes in dielectric nanoparticles. Nat Commun 2015;6:8069.
[112] Basharin AA, Kafesaki M, Economou EN, et al. Dielectric metamaterials with toroidal dipolar response. Phys Rev X 2015;5:011036.
[113] Li J, Shao J, Wang Y-H, Zhu M-J, Li J-Q, Dong Z-G. Toroidal dipolar response by a dielectric microtube metamaterial in the terahertz regime. Opt Express 2015;23:29138–44.
[114] Liu W, Zhang J, Miroshnichenko AE. Toroidal dipole-induced transparency in core-shell nanoparticles. Laser Photon Rev 2015;9:564–70.
[115] Zhang Q, Xiao JJ, Zhang XM, Han D, Gao L. Core-shell-structured dielectric-metal circular nanodisk antenna: gap plasmon assisted magnetic toroid-like cavity modes. ACS Photonics 2015;2:60–5.
[116] Li J, Zhang Y, Jin R, Wang Q, Chen Q, Dong Z. Excitation of plasmon toroidal mode at optical frequencies by angle-resolved reflection. Opt Lett 2014;39:6683–6.
[117] Wu PC, Hsu W-L, Chen WT, et al. Plasmon coupling in vertical split-ring resonator metamolecules. Sci Rep 2015;5:9726.
[118] Dong Z-G, Zhu J, Yin X, Li J, Lu C, Zhang X. All-optical Hall effect by the dynamic toroidal moment in a cavity-based metamaterial. Phys Rev B 2013;87:245429.
[119] Wu PR, Liao CY, Chen WT, et al. Horizontal toroidal response in three-dimensional plasmonic (Conference Presentation). Proc SPIE 2016;9921:992120–1.
[120] Liao CY, Chen MK, Huang Y-W, et al. Optical toroidal response in three-dimensional plasmonic metamaterial (Conference Presentation). Proc SPIE 2015;9547:954724.
[121] Tasolamprou AC, Tsilipakos O, Kafesaki M, Soukoulis CM, Economou EN. Toroidal eigenmodes in all-dielectric metamolecules. Phys Rev B 2016;94:205433.
[122] Xiang H, Ge L, Liu L, et al. A minimal discrete model for toroidal moments and its experimental realization. Phys Rev B 2017;95:045403.
[123] Heras JA. Electric and magnetic fields of a toroidal dipole in arbitrary motion. Phys Lett A 1998;249:1–9.
[124] Radescu EE, Vaman G. Toroid moments in the momentum and angular momentum loss by a radiating arbitrary source. Phys Rev E 2002;65:035601.
[125] Liu N, Giessen H. Coupling effects in optical metamaterials. Angew Chem Int Edit 2010;49:9838–52.
[126] Arima TH, Jung JH, Matsubara M, et al. Resonant magnetoelectric X-ray scattering in $GaFeO_3$: observation of ordering of toroidal moments. J Phys Soc Jpn 2005;74:1419–22.
[127] Collins SP, Laundy D, Connolley T, et al. On the possibility of using X-ray Compton scattering to study magnetoelectrical properties of crystals. Acta Crystallogr A 2016;72:197–205.
[128] Rikken GLJA, Raupach E. Observation of magneto-chiral dichroism. Nature 1997;390:493–4.
[129] Gupta M, Savinov V, Xu N, et al. Sharp toroidal resonances in planar terahertz metasurfaces. Adv Mater 2016;28:8206–11.
[130] Wei L, Xi Z, Bhattacharya N, Urbach HP. Excitation of the radiationless anapole mode. Optica 2016;3:799.
[131] Gu L, Sigle W, Koch CT, et al. Resonant wedge-plasmon modes in single-crystalline gold nanoplatelets. Phys Rev B 2011;83:195433.
[132] Ögüt B, Talebi N, Vogelgesang R, Sigle W, Van Aken PA. Toroidal plasmonic eigenmodes in oligomer nanocavities for the visible. Nano Lett 2012;12:5239–44.
[133] García De Abajo FJ. Optical excitations in electron microscopy. Rev Mod Phys 2010;82:209–75.
[134] Guo S, Talebi N, Sigle W, et al. Reflection and phase matching in plasmonic gold tapers. Nano Lett 2016;16:6137–44.
[135] Ögüt B, Vogelgesang R, Sigle W, Talebi N, Koch CT, Van Aken PA. Hybridized metal slit eigenmodes as an illustration of Babinet's principle. ACS Nano 2011;5:6701–6.
[136] Talebi N. A directional, ultrafast and integrated few-photon source utilizing the interaction of electron beams and plasmonic nanoantennas. New J Phys 2014;16:053021.
[137] Talebi N, Ozsoy-Keskinbora C, Benia HM, Kern K, Koch CT, Van Aken PA. Wedge Dyakonov waves and Dyakonov plasmons in topological insulator Bi_2Se_3 probed by electron beams. ACS Nano 2016;10:6988–94.

[138] Devaney AJ, Wolf E. Radiating and nonradiating classical current distributions and the fields they generate. Phys Rev 1973;8:1044–7.
[139] Devaney AJ, Wolf E. Multipole expansions and plane wave representations of the electromagnetic field. J Math Phys 1974;15:234–44.
[140] Wolf E, Habashy T. Invisible bodies and uniqueness of the inverse scattering problem. J Mod Opt 1993;40:785–92.
[141] Liu W, Zhang J, Lei B, Hu H, Miroshnichenko AE. Invisible nanowires with interfering electric and toroidal dipoles. Opt Lett 2015;40:2293–6.
[142] Gershtein SS, Ya B. Zel'dovich's contribution to modern particle physics. Phys-Usp 2004;47:845 and references within.
[143] Wood CS, Bennett SC, Cho D, et al. Measurement of parity nonconservation and an anapole moment in cesium. Science 1997;275:1759–63.
[144] Gao Y, Ho CM, Scherrer RJ. Anapole dark matter at the LHC. Phys Rev D 2014;89:045006.
[145] Ho CM, Scherrer RJ. Anapole dark matter. Phys Lett B 2013;722:341–6.
[146] Grinblat G, Li Y, Nielsen MP, Oulton RF, Maier SA. Enhanced third harmonic generation in single germanium nanodisks excited at the anapole mode. Nano Lett 2016;16:4635–40.
[147] Naumov II, Bellaiche LM, Prosandeev SA, Ponomareva IV, Kornev IA. Ferroelectric nanostructure having switchable multi-stable vortex states. 2009; Patent Number: US7593250 B2.
[148] Gupta M, Singh R. Toroidal versus Fano resonances in high Q planar THz metamaterials. Adv Opt Mater 2016;4:2119–25.
[149] Fan Y, Zhang F, Fu Q, Wei Z, Li H. Controlling the toroidal excitations in metamaterials for high-Q response. arXiv:1609.05804 [physics.optics], 2016.
[150] Zhao J-F, Zhang Y-W, Li Y-H, Chen Y-Q, Fang K, He L. Wireless power transfer system based on toroidal metamaterials. Acta Phys Sin 2016;65:168801.
[151] Urban MJ, Dutta PK, Wang P, et al. Plasmonic toroidal metamolecules assembled by DNA origami. J Am Chem Soc 2016;138:5495–8.
[152] Totero Góngora JS, Miroshnichenko AE, Kivshar YS, Fratalocchi A. Anapole nanolasers for mode-locking and ultrafast pulse generation. Nat Commun 2017;8:15535.
[153] Huang Y-W, Chen WT, Wu PC, Fedotov VA, Zheludev NI, Tsai DP. Toroidal lasing spaser. Sci Rep 2013:3:1237.
[154] Naumov II, Bellaiche LM, Fu H. Unusual phase transitions in ferroelectric nanodisks and nanorods. Nature 2004;432:737–40.
[155] Li J, Xin X-X, Shao J, et al. From non- to super-radiating manipulation of a dipolar emitter coupled to a toroidal metastructure. Opt Express 2015;23:29384–9.
[156] Li J, Dong Z-G, Zhu M-J, Shao J, Wang Y-H, Li J-Q. Dual-band toroidal-dipole-induced transparency in optical regime. J Phys D: Appl Phys 2016;49:345104.
[157] Hellwarth RW, Nouchi P. Focused one-cycle electromagnetic pulses. Phys Rev E Stat Phys Plasmas Fluids Relat Interdiscip Topics 1996;54:889–95.
[158] Raybould TA, Fedotov V, Papasimakis N, Youngs I, Zheludev N. Focused electromagnetic doughnut pulses and their interaction with interfaces and nanostructures. Opt Express 2016;24:3150–61.
[159] Romming N, Kubetzka A, Hanneken C, Von Bergmann K, Wiesendanger R. Field-dependent size and shape of single magnetic skyrmions. Phys Rev Lett 2015;114:177203.
[160] Marrows CH. An inside view of magnetic skyrmions. Physics 2015;8:40.
[161] Boleininger A, Lake T, Hami S, Vallance C. Whispering gallery modes in standard optical fibres for fibre profiling measurements and sensing of unlabelled chemical species. Sensors 2010;10:1765–81.